Design and Implementation of a Leg-wheel robot: *Transleg*

Zhong Wei
School of Instrument Science and Engineering, Southeast University
Nanjing 210096, China
zwei371@163.com

Guangming Song[1]
School of Instrument Science and Engineering, Southeast University
Nanjing 210096, China
mikesong@seu.edu.cn

Guifang Qiao
School of Automation, Nanjing Institute of Technology
Nanjing 211167, China
qiaoguifang@126.com

Ying Zhang
School of Instrument Science and Engineering, Southeast University
Nanjing 210096, China
zhangying295@126.com

Huiyu Sun
School of Instrument Science and Engineering, Southeast University
Nanjing 210096, China
sunhuiyu2010@163.com

ABSTRACT

In this paper, the design and implementation of a novel leg-wheel robot called *Transleg* are presented. *Transleg* adopts the wire as the transmission mechanism to simplify the structure and reduce the weight. To the best knowledge of the authors, the wire-driven method has never been used in the leg-wheel robots, so it makes *Transleg* distinguished from the existing leg-wheel robots. *Transleg* possesses four transformable leg-wheel mechanisms, each of which has two active degrees of freedom in the legged mode and one in the wheeled mode. Two actuators driving each leg-wheel mechanism are mounted on the body, so the weight

[1] Corresponding author.

of the leg-wheel mechanism is reduced as far as possible, which contributes to improving the stability of the legged locomotion. Inspired by the quadruped mammals, a compliant spine mechanism is designed for *Transleg*. The spine mechanism is also actuated by two actuators to bend in the yaw and pitch directions. It will be beneficial to the turning motion in the legged and wheeled modes and the bounding gait in the legged mode. The design and kinematic analyses of the leg-wheel and spine mechanisms are presented in detail. To verify the feasibility of *Transleg*, a prototype is implemented. The experiments on the motions in the legged and wheeled modes, the switch between the two modes and the spine motions are conducted. The experimental results demonstrate the validity of *Transleg*.

Key words: *Transleg*, leg-wheel robot, wire-driven, transformable, spine.

1. INTRODUCTION

According to the counterparts in the nature, the legged robots have the potentials to negotiate the rough terrain agilely [1]. Some advanced legged robots have been designed to achieve this goal, such as BigDog [2], LittleDog [3], Spot and RoboSimian [4]. Although the wheeled robots cannot cross the rugged topography as the legged robots, they can perform high-speed, smooth and energy-efficient locomotion on the flat ground [5]. To combine the advantages of the legged and wheeled robots, various leg-wheel robots with different structures and dimensions are proposed. The leg-wheel robots can be classified into two categories according to the way in which the wheel function is integrated into the leg-wheel robots.

One category of leg-wheel robots owns the separate wheel mechanisms. That is to say, the traditional wheels can be seen in the robots. For example, PAW [6], Hylos [7], Walk'n Roll [8], Roller-Walker [9], MHT [10], ATHELET [11], AirHopper [12], HIT-HYBTOR [13], Rolling-wolf [14], RT-Mover [15], Zero Carrier [16], and LegVan [17] all have a wheel on the tip of each leg. NOROS [18] possesses a wheel on each shank,

and NOROS-Ⅱ [19] mounts the wheel on the tip of each thigh. A leg-wheel robot designed by L. Guo et al. has one wheel on the tip of the leg, one on the tip of the thigh and the other on the body [20]. Mounting the wheel on the leg will increase the weight of the leg and will lead to the instability of the legged locomotion. Therefore, a few robots only fix the wheels on the body. For instance, HyTRo-Ⅰ[21] possesses four wheels on the body. A Stair-Cleaning Robot proposed by L. Zhang et al. has four wheels distributed as HyTRo-Ⅰ [22]. Wheeleg owns two wheels on the rear of the body and two legs on the front, and it looks like a cart [23]. E. Ottaviano and P. Rea developed a leg-wheel robot with the structure similar to Wheeleg [24]. Mantis 2.0 is equipped with four wheels and two rotating legs [25]. The wheels of these robots are designed to be active or passive in the light of different requirements. The active wheels can increase the flexibility of wheeled locomotion, while the passive ones can lighten the weight of the robots. However, whether the wheels are active or passive, mounted on the leg or the body, the weight of the robot will be increased.

The other category of leg-wheel robots has the coupled leg-wheel mechanism, which couples the leg with the wheel in function or structure. The spoke wheel without rim is one kind of such mechanism, and it acts as a wheel on the level ground and a leg on the rugged one. Whegs series [26] and IMPASS [27] are two typical robots with such mechanisms. Although the leg-wheel mechanisms of Loper [28] and ASGUARD [29] seem to be different from the spoke wheel, they are similar in function. The other kind of coupled leg-wheel mechanism is the transformable leg-wheel, which can change between the legged and wheeled structures according to the terrain. Wheel Transformer [30], Quattroped [31], Turboquad [32], LEON [33] and PEOPLER-II [34] have diverse

transformable leg-wheels which transform in different ways. K. Tadakuma et al. [35] and Y. She et al. [36] also designed two leg-wheel robots with different transformable leg-wheels. Compared with the spoke wheel without rim, the transformable leg-wheel is more flexible, but the structure becomes more complex.

Transleg proposed in this paper adopts four transformable leg-wheels, and the wire-driven method is utilized to reduce the complexity of the structure. In addition, the use of the wire-driven method allows the heavy actuators to be located far from the leg-wheels, which is beneficial to the stability of the legged locomotion [37]. Because of the advantages, the wires have been applied to actuate many robots, like quadruped robot [38], bipedal robot [39], robot fish [40], continuum robot [41-45], hyper-redundant robot [46] and so on. Compared with the first category of leg-wheel robots, the structure of *Transleg* is simpler since it has no separate wheel mechanisms. *Transleg* owns two actuators for each leg-wheel, while some leg-wheel robots with spoke wheels, such as Whegs, Loper and ASGUARD, have only one actuator for each spoke wheel. However, Whegs, Loper and ASGUARD cannot select the contact points with the ground for the legs. To make up for this defect, IMPASS adds one actuator for each spoke, so four actuators are needed for each spoke wheel. Different from the legs of Wheel Transformer, Quattroped, Turboquad, PEOPLER-II and the robot proposed by Y. She et al., the legs of *Transleg* are inspired by the limbs of the quadruped mammals. However, they are much simplified, and only two pitch joins are reserved. The legs of LEON and the robot designed by K. Tadakuma et al. also mimic the biological legs, but the actuators are mounted on the legs, which leads to the instability of the legged locomotion. The

characteristics of some leg-wheel robots referenced in this paper and *Transleg* are listed in Table 1.

Inspired by the quadruped mammals in the nature, a compliant wire-driven spine mechanism is designed for *Transleg*. The spine mechanism is actuated by two actuators and can bend in the yaw and pitch directions. It will contribute to the turning motion and bounding gait in the legged mode. Some quadruped robots have introduced the spine mechanism to improve the locomotion performance, such as Cheetah-I [47], Cheetah-Cub-S [48], Bobcat [49], Lynx [50], and Kitty [51]. The spines of Cheetah-I, Lynx, and Kitty use wires as the transmission mechanism, the one of Cheetah-Cub-S uses rigid bars, and Bobcat adopts direct-drive method. Moreover, Cheetah-I, Bobcat and Lynx can just bend in the pitch direction, and Cheetah-Cub-S can only bend in the yaw direction. Though Kitty can bend in both two directions as *Transleg*, its spine mechanism is actuated by four actuators. The rest of this paper is organized as follows. Section 2 gives the detailed mechanical layouts of *Transleg*. Section 3 introduces the kinematic analyses. Section 4 presents the experimental validations. And the concluding remarks are given in Section 5.

Table 1. Characteristics of some leg-wheel robots referenced in this paper and *Transleg*

Name	n_A	n_{LD}	n_{WD}
PAW [6]	2	1	1
Hylos [7]	4	2	2
Walk'n Roll [8]	2/3	1/3	0/1
Roller-Walker [9]	3	3	0
MHT [10]	3	2	1
Zero Carrier [16]	1/2	1	0/1

LegVan [17]	3/4	2	1/2
NOROS [18]	4	3	1
NOROS-Ⅱ [19]	3/4	3	0/1
IMPASS [27]	4	4	1
Loper [28]	1	1	1
Wheel Transformer [30]	1	1	1
Quattroped [31]	3	2	1
Turboquad [32]	2	2	1
LEON [33]	4	4	2
Transleg	**2**	**2**	**1**

Note: n_A denotes the number of actuators for each leg-wheel, n_{LD} denotes the number of active DOFs (degrees of freedom) for the leg, n_{WD} denotes the number of active DOFs for the wheel. "/" denotes "or", indicating the leg-wheels of the robot have different numbers of actuators or DOFs.

2. MECHANICAL LAYOUTS

2.1. Overall Design

The prototype of *Transleg* in the legged and wheeled modes is shown in Fig. 1. The robot has four transformable leg-wheel mechanisms at the corners of the body. Therefore, *Transleg* can perform as a quadruped robot in the legged mode, and a four-wheel vehicle in the wheeled mode. The body consists of two parts which are connected by a spine mechanism. The introduction and creation of the spine mechanism are inspired by the quadruped mammals in the nature. The spine plays a significant role in the locomotion of these animals, such as self-balance, bounding gait and so on. Therefore, it is valuable to study on integrating the spine motions into the locomotion of the quadruped robot. Moreover, the spine can improve the turning performance in the wheeled mode.

Due to the open architecture of *Transleg*, the controller, sensors, battery and some other functional modules can be expediently integrated when needed. *Transleg* is driven by ten Dynamixel MX-64R actuators, which are controlled through the RS-485 communication. The wires used as the transmission mechanism are steel rope and PE nylon rope, which can be extended so little that they are assumed to be rigid. Now most components of *Transleg* are made from the toughened resin or cut from the carbon fiber composite material, the weight is 2.245kg, and the dimensions are 331.20mm×252.00mm×195.42mm (length×width×height). The leg-wheel and spine mechanisms are the two main mechanisms of *Transleg*, which will be carefully described later on.

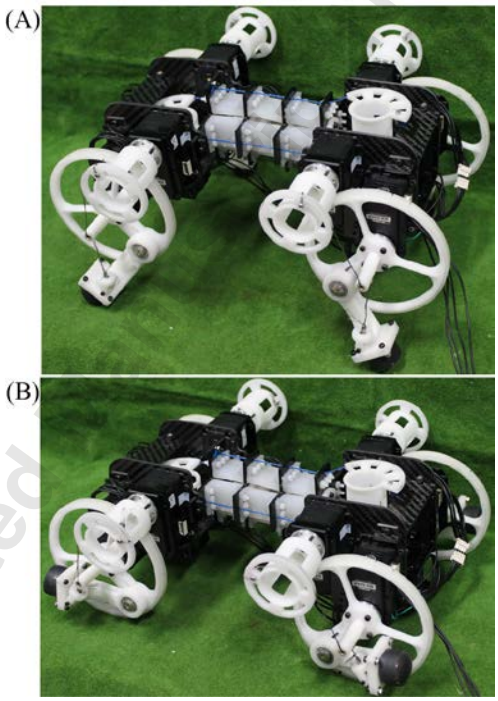

Fig. 1 Prototype of *Transleg* in the (A) legged and (B) wheeled modes

2.2. Design of Leg-Wheel Mechanism

As shown in Fig. 2(A), the two actuators driving the leg-wheel mechanism are mounted on the body, so the weight of the leg-wheel mechanism is largely reduced. To make the spine mechanism easy to understand, it is introduced in several parts:

a. Hip joint. The output shaft of actuator 1 is connected with the thigh, forming the hip joint. The thigh has a circle rim which is supported by two spokes and the thigh, and the hip joint is just at the center of the rim.

b. Knee joint. The shank is jointed with the thigh by a docking assembly, forming the knee joint. At the joint, a thrust ball bearing is used to decrease the friction and a torsion spring is mounted. The two ends of the torsion spring are respectively fixed at the thigh and the shank, so the knee joint can keep an initial angle.

c. Transmission mechanism for knee joint. A turnplate is connected with the output shaft of actuator 2, and one end of a wire is fixed on the turnplate. The wire crosses a hole whose entrance is at the center of the rim of the thigh. The other end of the wire is fixed on a rotary assembly which is mounted on the shank with a revolute pair. The foot is mounted at the end of the shank.

d. Rotary assembly. The rotary assembly is composed of a bearing pedestal, a flange bearing and a dowel. One end of the wire is fixed on the dowel, which crosses a flange bearing. The flange bearing is fixed on the bearing pedestal, which is mounted on the shank with a revolute pair. The dowel will rotate when the wire is twisted in the wheeled locomotion. The revolute pair can make the dowel in a line with the wire.

e. Legged mode. The leg-wheel mechanism is in the legged mode when the shank is out of the rim of the thigh, as shown in Fig. 2(A). By actuating the two actuators

mounted on the body coordinately, the hip and knee joints can rotate in the certain tracks, and the leg-wheel mechanism can perform the legged locomotion.

f. Wheeled mode. The leg-wheel mechanism can easily transform from the legged mode to the wheeled mode by actuating actuator 2 to pull the shank in the rim of the thigh, as shown in Fig. 2(B). In the wheeled mode, by keeping the knee joint static and driving actuator 1, the leg-wheel mechanism can perform the wheeled locomotion. In the wheeled locomotion, the hole rotates together with the rotating rim, and the turnplate keeps stationary.

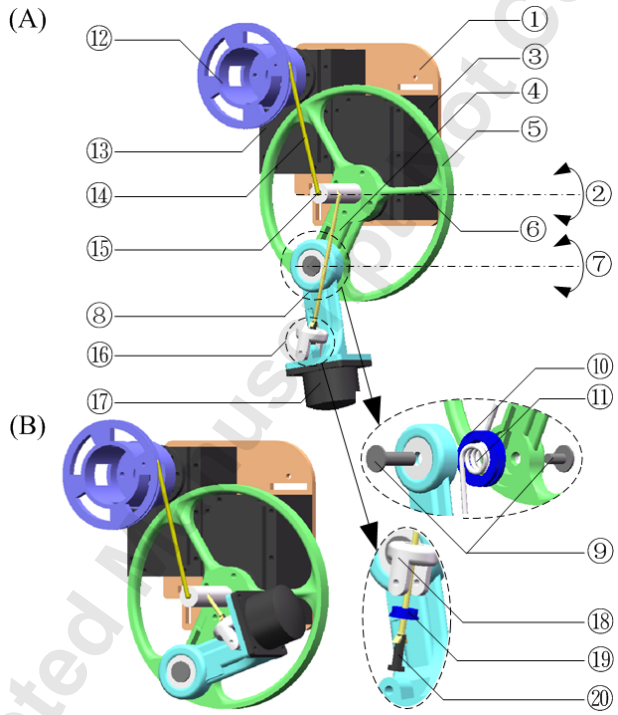

Fig. 2 Schematic diagram of the leg-wheel mechanism in the (A) legged and (B) wheeled modes. The numbers denote: ① body, ② hip joint, ③ actuator 1, ④ thigh, ⑤ rim, ⑥ spoke, ⑦ knee joint, ⑧ shank, ⑨ docking assembly, ⑩ thrust ball bearing, ⑪ torsion spring, ⑫ turnplate, ⑬ actuator 2, ⑭ wire, ⑮ hole, ⑯ rotary assembly, ⑰ foot, ⑱ bearing pedestal, ⑲ flange bearing, ⑳ dowel

2.3. Design of Spine Mechanism

As shown in Fig. 3, the spine mechanism is driven by two actuators which are respectively mounted on the front and rear bodies. To make the spine mechanism easy to understand, it is introduced in several parts:

a. Mechanism for bending in pitch direction. The pitch actuator drives the spine to bend in the pitch direction, and it is mounted on the front body. The output shaft of the pitch actuator is connected with the pitch turnplate. The pitch turnplate has two fan-shaped wire spools on which two wires allocated up and down are mounted. The wires cross the guide holes on the spine joints, and the end of them are fixed on the tail end of the spine joints.

b. Mechanism for bending in yaw direction. The yaw actuator drives the spine to bend in the yaw direction, and it is mounted on the rear body. The output shaft of the yaw actuator is connected with the yaw turnplate. Two wires allocated left and right are mounted on the semicircular wire spool of the yaw turnplate. The wires cross the guide holes on the spine joints, and the end of them are fixed on the head end of the spine joints.

c. Spine joints. The tail and head ends of the spine joints are respectively fixed on the rear and front bodies. The spine joints are made up of vertebras and silicon pieces. The silicon pieces work as the intervertebral disks in the mammal. Between two vertebras, there are four silicon pieces. To see the inner structure of the spine joints, some silicon pieces are made transparent. The wires and silicon pieces are symmetrically allocated around the ball joints. In addition, the number of joins can be determined as needed. There are three ball joints in Fig. 3.

d. Bend in the yaw and pitch directions. When the pitch turnplate is driven to rotate clockwise or anticlockwise by the pitch actuator, the wire allocated up or down is pulled, and then the spine joints bend up or down. That is to say, *Transleg* bends in the pitch direction. Likewise, *Transleg* bends in the yaw direction, when the yaw turnplate is driven.

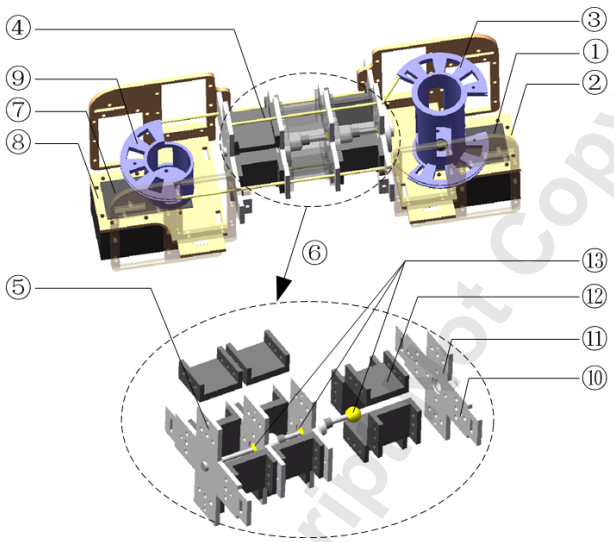

Fig. 3 Schematic diagram of the spine mechanism. The numbers denote: ① pitch actuator, ② front body, ③ pitch turnplate, ④ wire, ⑤ tail end, ⑥ spine joints, ⑦ yaw actuator, ⑧ rear body, ⑨ yaw turnplate, ⑩ head end, ⑪ vertebra, ⑫ silicon piece, ⑬ ball joints

3. KINEMATIC ANALYSES

3.1. Motion of Leg-Wheel Mechanism

Transleg is mainly propelled by the four leg-wheel mechanisms, and it can perform legged and wheeled locomotion. In the legged mode, *Transleg* works like a quadruped robot, which has the hip and knee joints in each leg. Therefore, all the typical gait of the quadruped robot, such as walking, trotting, bounding, pacing and galloping, can be achieved.

A. Motion tracks of hip and knee joints

In this paper, the trotting gait is applied to *Transleg*, and the motion tracks of the hip and knee joints are planned using the method proposed in [52]. With this gait, the diagonal legs of *Transleg* keep synchronous. If two synchronous legs are in the swing phase or the beginning of the swing phase, the other two must be in the stance phase or the beginning of the stance phase. In the swing phase, the hip joints move from back (PEP, short for posterior extreme position) to front (AEP, short for anterior extreme position), and the knee joints move to lift the shank up and then down. When the legs are in the extreme position, *Transleg* touches the ground with four legs, which means *Transleg* is in the balanced state. In the stance phase, the hip joints move from front to back, and the knee joints keep motionless. To simplify the control method, the cosine signal rather than the CPG (central pattern generator) is employed to control the motion of the hip joint. Then the motion track of the hip joint is described as

$$\begin{cases} \theta_{\mathrm{HR}}(t) = a\dfrac{A_{\mathrm{H}}}{2}(\cos\dfrac{2\pi}{T_1}t - 1) \\ a = \begin{cases} 1 & (\mathrm{FL},\ \mathrm{FR}) \\ -1 & (\mathrm{HL},\ \mathrm{HR}) \end{cases} \end{cases} \tag{1}$$

where θ_{HR}, A_{H} and T_1 are respectively the angle displacement, swing amplitude, and swing cycle of the hip joint. FL, HR, HL and FR denote the front-left, hind-right, hind-left, and front-right leg-wheel respectively. The motion track of the knee joint is slightly modified on the basis of the one in [49], and is defined as

Journal of Mechanisms and Robotics. Received October 20, 2016;
Accepted manuscript posted June 9, 2017. doi:10.1115/1.4037018

$$\begin{cases} \theta_{KR}(t) = \begin{cases} b\left(\frac{A_H}{2} - \left|\left|\theta_{HR}(t)\right| - \frac{A_H}{2}\right|\right)k(t) & \text{(swing phase)} \\ 0 & \text{(stance phase)} \end{cases} \\ k(t) = 2\frac{A_K}{A_H}\left(1 + \frac{2}{A_H}\left|\left|\theta_{HR}(t)\right| - \frac{A_H}{2}\right|\right) \\ b = \begin{cases} 1 & \text{(FR, HL)} \\ -1 & \text{(FL, HR)} \end{cases} \end{cases} \quad (2)$$

where θ_{KR} and A_K are respectively the angle displacement and swing amplitude of the knee joint.

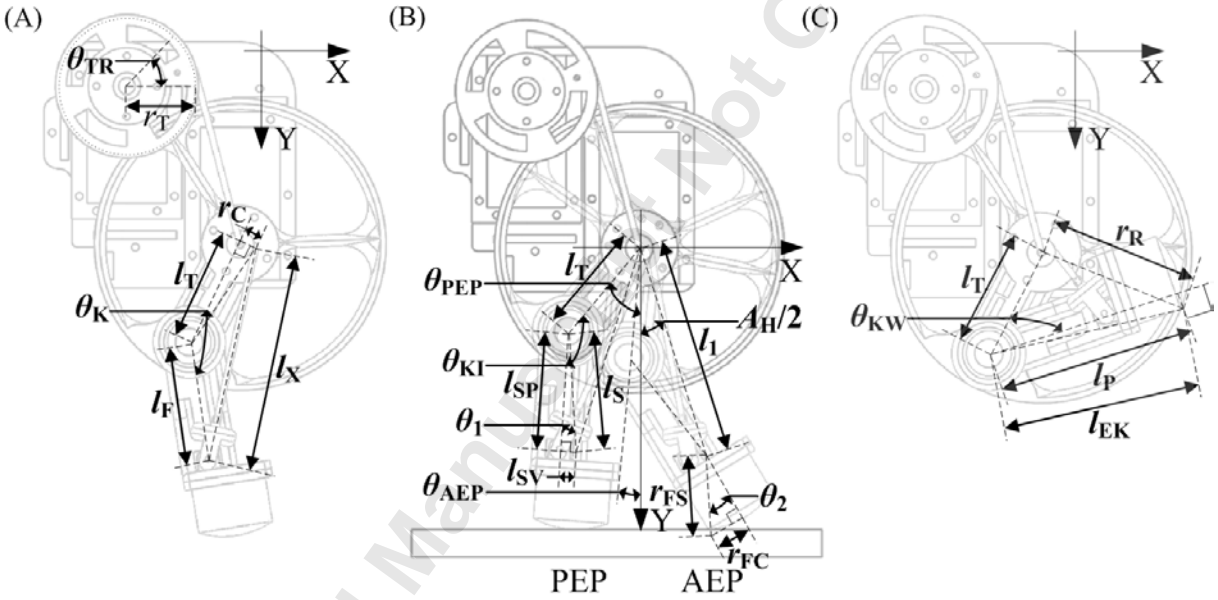

Fig. 4 Geometries of leg-wheel mechanism for explaining (A) the relation between the rotation angle of turnplate and the angle of knee joint, (B) the angles of hip joint in anterior extreme position and posterior extreme position, and (C) the angle of knee joint in the wheeled mode

B. Angle displacement of actuator driving knee joint

Because the knee joint is driven by the turnplate through wire, the relation between the rotation angle θ_{TR} of turnplate and the angle θ_K of knee joint should be

derived. According to the geometries of the leg-wheel mechanism in Fig. 4(A), the relation between θ_{TR} and θ_K is

$$\begin{cases} l_{XI} = \sqrt{r_C^{\,2} + l_T^{\,2} + l_F^{\,2} - 2\sqrt{r_C^{\,2} + l_T^{\,2}}\, l_F \cos(\theta_{KI} - \arctan\dfrac{r_C}{l_T})} \\ l_X = \sqrt{r_C^{\,2} + l_T^{\,2} + l_F^{\,2} - 2\sqrt{r_C^{\,2} + l_T^{\,2}}\, l_F \cos(\theta_K - \arctan\dfrac{r_C}{l_T})} \\ \theta_{TR} = c\dfrac{l_{XI} - l_X}{r_T} \\ c = \begin{cases} 1 & \text{(FR,HL)} \\ -1 & \text{(FL,HR)} \end{cases} \end{cases} \tag{3}$$

where r_C is the radius of the cylinder at the hip joint, l_T is the distance from the hip joint to the knee joint, θ_{KI} is the initial angle of the knee joint, l_F is the distance from the knee joint to the point where the rotary assembly is fixed, and r_T is the radius of the turnplate. In addition, θ_{KR} and θ_K satisfy the following relation

$$\theta_K = \theta_{KI} - |\theta_{KR}| \tag{4}$$

C. Position of hip joint in AEP and PEP

In the legged locomotion, the leg-wheel swings between the AEP (anterior extreme position) and the PEP (posterior extreme position), as shown in Fig. 4(B). When the leg-wheels are in the two positions, the distances from the four hip joints to the ground are the same, and *Transleg* is in the balanced state. To keep smooth moving, the quadruped robot usually starts from the balanced state, so the angle θ_{HAEP} of the hip joint in the AEP and the one θ_{HPEP} in the PEP should be figured out. According to the geometries in Fig. 4(B), θ_{HAEP} and θ_{HPEP} are expressed as

$$\begin{cases} \theta_{HAEP} = \arcsin\dfrac{l_S \sin(\theta_{KI} - \theta_1)}{l_1} - \dfrac{A_H}{2} \\ \theta_{HPEP} = \theta_{HAEP} + A_H \end{cases} \tag{5}$$

where l_S is the distance from the knee joint to the center of the sphere surface of the foot. l_S and θ_1 are given by

$$\begin{cases} l_S = \sqrt{{l_{SP}}^2 + {l_{SV}}^2} \\ \theta_1 = \arctan(\dfrac{l_{SV}}{l_{SP}}) \\ l_1 = \sqrt{{l_T}^2 + {l_S}^2 - 2 l_T l_S \cos(\theta_{KI} - \theta_1)} \end{cases} \tag{6}$$

where l_{SP} and l_{SV} are respectively the projections of l_S to the broadside and base of the shank. It is worth noting that the calculations of θ_{HAEP} and θ_{HPEP} are on the basis of the hypothesis that the leg-wheels touch the ground with the sphere surface of the foot. Hence, the swing amplitude of the hip joint A_H should satisfy

$$\begin{cases} A_H \le 2(\arcsin \dfrac{l_S \sin(\theta_{KI} - \theta_1)}{l_1} - \pi + \theta_{KI} + \theta_2) \\ \theta_2 = \arcsin \dfrac{r_{FC}}{r_{FS}} \end{cases} \tag{7}$$

where r_{FC} is the radius of the cylinder of the foot, and r_{FS} is the radius of the sphere surface of the foot.

D. Wheeled locomotion

In the wheeled locomotion, only the hip joint is actuated, and the knee joint maintain the angle θ_{KW}. Therefore, the motion tracks of the hip and knee joints are

$$\begin{cases} \theta_{HR}(t) = \dfrac{2\pi}{T_2} t \\ \theta_{KR} = 0 \end{cases} \tag{8}$$

where T_2 is the rotation cycle of the hip joint. According to the geometries in Fig. 4(C), θ_{KW} is described as

$$\theta_{KW} = \arccos \frac{{l_{EK}}^2 + {l_T}^2 - {r_R}^2}{2 l_{EK} l_T} - \arccos \frac{l_P}{l_{EK}} \tag{9}$$

Where l_{EK} is the distance from the knee joint to the point where the edge of the foot overlaps with the rim of the thigh, r_R is the radius of the rim of the thigh, and l_P is the distance from the knee joint to the plane in which the circle edge of the foot is.

E. Switch between legged and wheeled modes

To adequately take advantage of the mobility performance, *Transleg* should transform between the legged and wheeled modes according to the terrain. The selection of the transformation position is important to the transforming process. As noted above, *Transleg* is in the balanced state in the extreme position. Therefore, the extreme position is set as the transformation position in this paper. When *Transleg* transforms from the legged locomotion to the wheeled motion, the thigh keeps motionless in the extreme position and the shank moves until the foot is inside the rim of thigh. The angle displacement of the turnplate can be figured out by replacing θ_K with θ_{KW} in (3). When *Transleg* performs the inverse transformation, the thigh stops in the extreme position and the shank moves until the knee joint is in the initial angle θ_{KI}. The angle displacement of the turnplate is just the opposite value of the one obtained when *Transleg* transforms from the legged mode to the wheeled mode.

3.2. Motion of Spine Mechanism

The spine mechanism is driven to bend in the yaw and pitch directions by two turnplates mounted on the output shafts of the actuators through wire. To control the spine mechanism well, the relations between the bending angles of spine joints in the yaw and pitch directions and the rotation angles of the actuators need be figured out. The motion of the spine mechanism is driven by pulling the wires using the wire spool of the turnplate. Therefore, when the spine mechanism bends, the decrement of the length of the

Journal of Mechanisms and Robotics. Received October 20, 2016;
Accepted manuscript posted June 9, 2017. doi:10.1115/1.4037018

wire in the spine joints is equal to the length of the wire which the wire spool takes back. Because the wires are symmetrically allocated around the joints, the variations of the lengths of the wires in the spine joints are identical when the spine mechanism bends in the yaw and pitch directions with the same angle. Moreover, the distances of the adjacent vertebras are the same, and the silicon pieces are supposed to be identical. Hence, the bending angles of all the ball joints are the same, and the variations of the lengths of the wires between any two adjacent vertebras are equal.

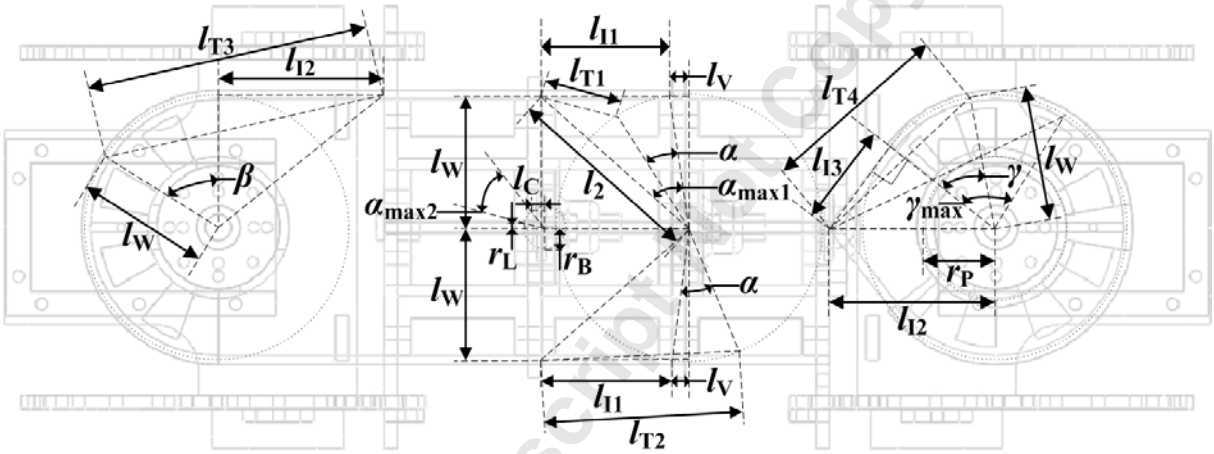

Fig. 5 Geometries of spine mechanism for explaining (1) the relation between the bending angle of *Transleg* in the yaw direction and the rotation angle of the yaw actuator, and (2) the relation between the bending angle of *Transleg* in the pitch direction and the rotation angle of the pitch actuator

A. Decrement and increment of length of wire in spine joints

According to the geometries in Fig. 5, the relation between the decrement l_{DE} of the length of the wire in the spine joints and the bending angle α of one joint is

$$\begin{cases} l_{DE} = 3(l_{I1} - l_{T1}) \\ l_{T1} = \sqrt{l_2^{\,2} + l_W^{\,2} + l_V^{\,2} - 2l_2\sqrt{l_W^{\,2} + l_V^{\,2}}\cos(\alpha_{max1} - \alpha)} \end{cases} \tag{10}$$

where l_{I1} and l_{T1} are respectively the lengths of the wires between the adjacent vertebras before and after the spine joints bend, l_V is the distance from rotation center of the ball

joint to the plane of the vertebral, and l_W is the distance from rotation center of the ball joint to the wire. α_{max1} is the maximum bending angle of spine joint, exceeding which the length of the wire between the adjacent vertebras increases. l_2 and α_{max1} are given by

$$\begin{cases} l_2 = \sqrt{{l_W}^2 + (l_{I1} + l_V)^2} \\ \alpha_{max1} = \arctan\dfrac{l_{I1} + l_V}{l_W} - \arctan\dfrac{l_V}{l_W} \end{cases} \tag{11}$$

The maximum bending angle is also limited by the maximum angle α_{max2} that the ball joint can rotate.

$$\alpha_{max2} = \frac{\pi}{2} - \arcsin\frac{l_C}{r_B} - \arcsin\frac{r_L}{r_B} \tag{12}$$

where l_C is the thickness of the cover which prevents the ball from being out, r_B is the radius of the ball, and r_L is the radius of the link of the ball joint. The maximum bending angle α_{max} is the smaller one between α_{max1} and α_{max2}. When one ball joint bends with the angle α, the increment l_{IN} of the length of the wire in the spine joints is

$$\begin{cases} l_{IN} = 3(l_{T2} - l_{I1}) \\ l_{T2} = \sqrt{{l_2}^2 + {l_W}^2 + {l_V}^2 - 2l_2\sqrt{{l_W}^2 + {l_V}^2}\cos(\alpha_{max1} + \alpha)} \end{cases} \tag{13}$$

where l_{T2} is the length of the wire between the adjacent vertebras after the spine joints bend.

B. Length of wire taken back and let out by yaw and pitch turnplates

For the semicircular yaw turnplate, when it rotates with the angle β ($\beta \le \pi/2$), the length l_{TB1} of the wire taken back is

$$\begin{cases} l_{TB1} = l_{T3} - l_{I2} \\ l_{T3} = \sqrt{{l_{I2}}^2 + 2{l_W}^2 - 2l_W\sqrt{{l_W}^2 + {l_{I2}}^2}\cos(\arctan\dfrac{l_{I2}}{l_W} + \beta)} \end{cases} \tag{14}$$

where l_{T3} and l_{I2} are respectively the lengths of the wires between the turnplate and the spine joints after and before rotating. The length l_{LO1} of the wire let out is

$$l_{LO1} = \beta l_W \tag{15}$$

For the fan-shaped pitch turnplate, when it rotates with the angle γ, whose range is

$$\gamma \le \pi - \arcsin\frac{r_P}{l_{I2}} - \arcsin\frac{r_P}{l_W} - \arccos\frac{l_W}{l_{I2}} \tag{16}$$

the length l_{TB2} of the wire taken back is

$$\begin{cases} l_{TB2} = l_{T4} - l_{I3} \\ l_{T4} = \sqrt{{l_{I2}}^2 + {l_W}^2 - 2 l_{I2} l_W \cos(\arccos\frac{l_W}{l_{I2}} + \gamma)} \\ l_{I3} = \sqrt{{l_{I2}}^2 - {l_W}^2} \end{cases} \tag{17}$$

where r_P is the radius of the pedestal of the turnplate, and l_{T4} and l_{I3} are respectively the lengths of the wires between the turnplate and the spine joints after and before rotating. The length l_{LO2} of the wire let out is

$$l_{LO2} = \gamma l_W \tag{18}$$

C. Relation between bending angle of spine and rotation angles of actuators

Because l_{DE} is equal to l_{TB1} and l_{TB2}, the relations between the bending angle α_S (α_S=3α) in the yaw and pitch directions and the rotation angles of the actuators (β and γ) can be obtained, combining (10), (14) and (17). It should be noted that the decrement l_{DE} of the length of the wire in the spine joints is a little smaller than the increment l_{IN}. To make the spine mechanism work normally, the length of the wire let out should be longer than the one taken back. Therefore, the yaw and pitch turnplates are designed to be semicircular or fan-shaped.

4. SIMULATION VALIDATIONS

The simulations were done to verify the validity of the theory of the leg-wheel motion and the feasibility of the design of the leg-wheel mechanism. In the simulation, *Transleg* performed legged locomotion for five gait cycles, transformation from legged to wheeled mode, wheeled locomotion for one cycles, transformation from wheeled to legged mode, and legged locomotion for five gait cycles in turn. To avoiding the complex wire simulation, the control signals were directly applied to the hip and knee joints. What's more, the control signals needed in the simulation are the angle displacement relative to the initial position. The tracks of the hip and knee joints in (1) and (2) start from the extreme position where *Transleg* is in the balanced state. Hence, the extreme position is set as the initial state as well as the transformation position for *Transleg*. The control signals and some necessary parameters can be obtained by the equations in the previous section. The values of the geometries of *Transleg* are shown in Table 1.

Table 2. Values of the geometries of *Transleg*

Name	r_C	l_T	l_F	r_T	l_S	l_{SP}	l_{SV}	r_{FC}	r_{FS}	l_{EK}
Value (mm)	5.00	40.00	43.00	24.20	40.58	40.13	6.00	13.50	31.87	69.41
Name	r_R	l_P	l_{I1}	l_V	l_W	l_C	r_B	r_L	l_{I2}	r_P
Value (mm)	53.00	69.00	29.56	4.00	30.00	3.00	4.80	1.50	37.66	16.00

In this simulation, θ_{KI} is set as 140°, so A_H is not larger than 19° according to (7). Set A_H as 18°, and θ_{HAEP} and θ_{HPEP} are calculated as 15.44° and 33.44 according to (5). At t=0 in (1), the FL and HR leg-wheels are in the PEP, and the FR and HL ones are in the AEP. Set the hip and knee joints of the four leg-wheels of *Transleg* with the corresponding initial angles. A_K, T_1 and T_2 are set as 10°, 0.5s and 2s. In addition, θ_{KW} is

43.23°, and the time for the mode transformation is set as 2s. Therefore, the control signals directly applied on the hip and knee joints of the four leg-wheels can be achieved through (1) and (2). They are shown in Fig. 6. The snapshots of the simulation video using these control signals are shown in Fig. 7. The simulation results show that the control signals and parameters obtained pursuant to the equations in the previous section are right, and the leg-wheel mechanism can work well.

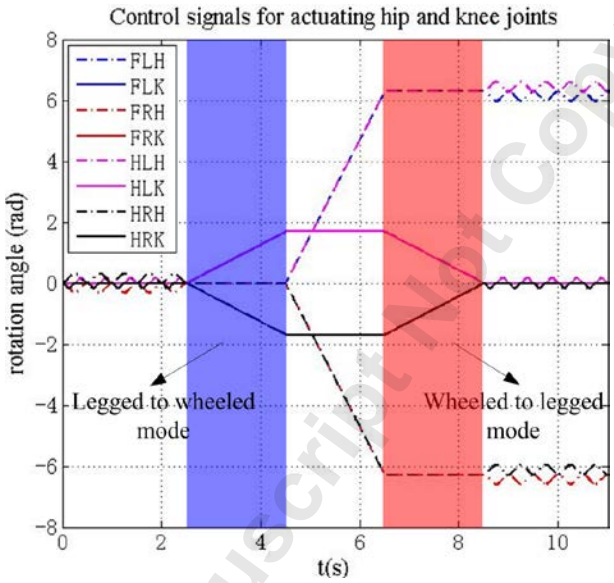

Fig. 6 Control signals actuating *Transleg* to perform legged and wheeled locomotion and switch between the two locomotion modes (FLH, FRH, HLH and HRH respectively denote hip joint of front-left, front-right, hind-left and hind-right leg-wheel; FLK, FRK, HLK and HRK respectively denote knee joint of front-left, front-right, hind-left and hind-right leg-wheel.)

Journal of Mechanisms and Robotics. Received October 20, 2016;
Accepted manuscript posted June 9, 2017. doi:10.1115/1.4037018

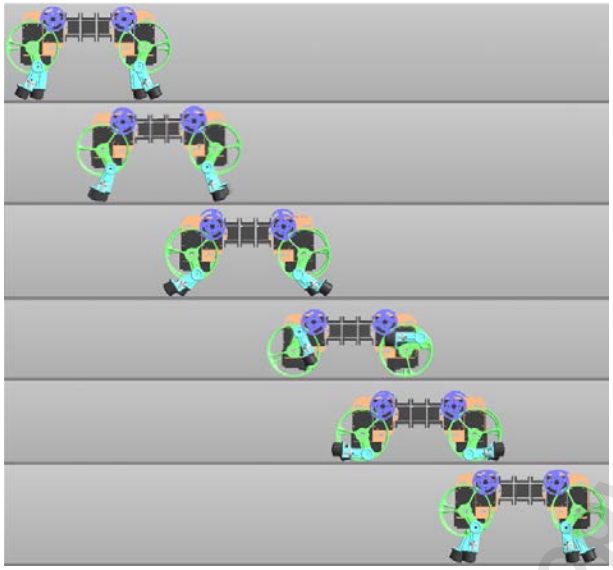

Fig. 7 Snapshots of *Transleg* performing legged, wheeled and transformation motion in the simulation (the video can be found at VideoLink)

5. EXPERIMENTAL VALIDATIONS

To further validate the effectiveness of the design of *Transleg*, two experiments on the motions of the prototype were conducted. Currently, *Transleg* is controlled by the program running on an external laptop through a RS-485 serial connection, and the power is provided by an external power supply.

5.1. Leg-Wheel Motions

In one experiment, *Transleg* was controlled to do the legged locomotion, legged to wheeled mode motion, forward and backward wheeled locomotion, wheeled to legged mode motion and legged locomotion successively. The actuators used in the prototype can work in three modes: wheeled, joint and multi-turn modes. Only the wheeled and joint modes are used here. In the wheeled mode, the actuators are controlled by assigning the moving speed and direction and can run endlessly. While they are controlled through the absolute angle position and have an operating angle range of 360° in the joint mode.

Therefore, the knee joint of the prototype can be controlled in the joint mode using the signal obtained by (2) after mapping to the rotation angle of the turnplate by (3) and adding the initial angle. The initial angle is the angle position of the corresponding actuator when *Transleg* is in the extreme position. The hip joint in the legged locomotion can be controlled using the track in (1) after adding the initial angle in the joint mode, while it needs to be controlled in the wheeled mode by specifying the moving speed. The experimental results are shown in Fig. 8.

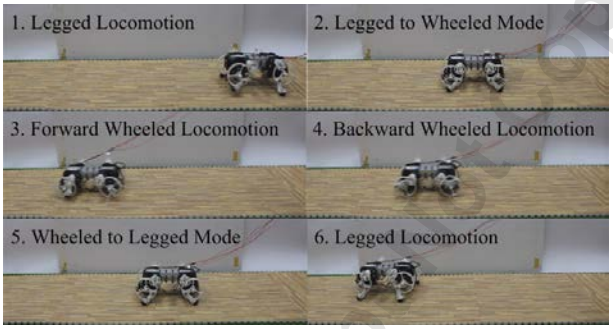

Fig. 8 Snapshots of *Transleg* performing legged, wheeled and transformation motion in the experiment (the video can be found at VideoLink)

5.2. Spine Motions

In the other experiment, *Transleg* was controlled to bend the spine without any leg-wheel motion. Pursuant to (11), (12) and the geometry values in Table. 1, the maximum bending angle α_{max} is 33.1°. When each ball joint rotates 33.1°, l_{DE} in (10) is 42.1mm. In addition, the maximum of β is 90° and that of γ is 85.4°. When they are in the maximum angles, the lengths of the wire taken back are respectively 36.3mm and 36.7mm, and the ball joint rotates 26.1° and 26.4°. Therefore, the maximum rotation angle of each ball joint is 26.1° in the yaw direction and 26.4° in the pitch direction. That is to say, *Transleg* can bend with the maximum angle 78.3° in the yaw direction and

79.2° in the pitch direction. Set the rotation angle of each ball joint 0~26.1°, and then the bending angle of the spine joins is 0~78.3°.

According to (10), (13), (14), (17) and (18), the relations between the bending angles of spine joints in yaw and pitch directions and the rotation angles of actuators, the increments and decrement of wire in the spine joints, and the length of wire let out by the yaw actuator and the pitch actuator can be figured out, as shown in Fig. 9. The decrement of the length of the wire (lDE) in the spine joints is smaller than the increment (lIN), and the difference is incremental with the increasing bending angle. This will cause the spine mechanism to fail to work. To deal with this problem, the yaw and pitch turnplates are designed to be semicircular or fan-shaped, which makes the turnplates let out longer wire than take back. As shown in Fig. 9, the wires let out by the turnplates (lLO1 and lLO2) are obviously longer than that lIN needs when the bending angle is big. In fact, when the bending angle is small, the wires let out by the turnplates are a little shorter than 0.04mm, which is small enough to be ignored. In this experiment, the yaw and pitch turnplates were actuated to rotate with different angles in two directions relative to the initial position where the spine is straight. The experimental results of the spine motion are shown in Fig. 10. The angles in this figure were measured with a protractor when *Transleg* was kept static. The results show that the turnplates collided with each other when *Transleg* bended with 45°, which is the actual maximum bending angle in the yaw direction.

Journal of Mechanisms and Robotics. Received October 20, 2016;
Accepted manuscript posted June 9, 2017. doi:10.1115/1.4037018

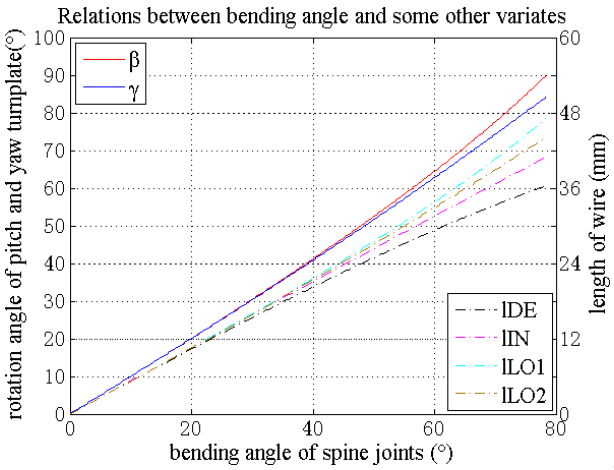

Fig. 9 Relations between the bending angles of spine joints in yaw and pitch directions and the rotation angles of actuators, the increments and decrements of wires in the spine joints, and the length of wire let out by the yaw actuator and the pitch actuator (solid lines and dotted lines are respectively relative to the left and right coordinates)

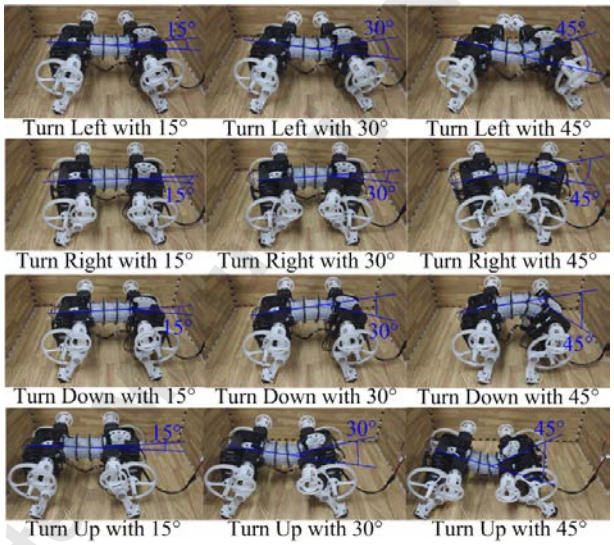

Fig. 10 Snapshots of *Transleg* performing spine motion (the video can be found at VideoLink)

6. CONCLUSIONS

Transleg proposed in this paper is a wire-driven leg-wheel robot. The leg-wheel mechanism is its main propelling mechanism, and it can transform between the legged and wheeled modes. Only two actuators are used to actuate each leg-wheel, which has the

hip and knee joints in the legged mode and the active revolution joint in the wheeled mode. Hence, *Transleg* can perform almost all the legged and wheeled locomotion. The spine mechanism is its one characteristic, and it can bend in the yaw direction with the maximum angle 45°, and in the pitch direction with 79.2°. The spine mechanism adopts the ball joint, whose number is extensible. In the present prototype, three ball joints exist. The experiments on the trotting gait and spine motion are conducted, and the results demonstrate the validity of *Transleg*. In the future, we will further optimize the structure of *Transleg*, study on its multi-mode locomotion and apply the advanced control method to it.

ACKNOWLEDGMENT

The research reported in this paper was conducted at the Robotic Sensor and Control Lab, School of Instrument Science and Engineering, Southeast University, Nanjing, Jiangsu, China. The authors thank all the members of the lab for their great supports.

FUNDING

This work is partially supported by Nature Science Foundation of China under Grant #61375076, and Jiangsu Provincial Key Laboratory of Remote Measurement and Control Technology under Grant #2242015k30005.

REFERENCES

[1] Ajallooeian, M., Pouya, S., Sproewitz, A., and Ijspeert, A., J., 2013, "Central pattern generators augmented with virtual model control for quadruped rough terrain locomotion," *Robotics and Automation (ICRA), 2013 IEEE International Conference on*, IEEE, pp, 3321-3328. DOI: 10.1109/ICRA.2013.6631040

[2] Wooden, D., Malchano, M., Blankespoor, K., Howard, A., Rizzi, A., A., and Raibert, M., 2010, "Autonomous navigation for BigDog," *Robotics and Automation (ICRA), 2010 IEEE International Conference on*, IEEE, pp. 4736-4741. DOI: 10.1109/ROBOT.2010.5509226

[3] Zucker, M., Ratliff, N., Stolle, M., Chestnutt, J., Bagnell, J., A., Atkeson, C., J., and Kuffner, J., 2011, "Optimization and learning for rough terrain legged locomotion," The International Journal of Robotics Research, **30**(2), pp. 175-191. DOI: 10.1177/0278364910392608

[4] Satzinger, B., W., Lau, C., Byl, M., and Byl, K., 2015, "Tractable locomotion planning for RoboSimian," The International Journal of Robotics Research, **34**(13), pp. 1541-1558. DOI: 10.1177/0278364915584947

[5] Morin, P., and Samson, C., 2008, *Springer Handbook of Robotics*, Springer Berlin Heidelberg, Chap. E. ISBN:9783540239574

[6] Sharf, I., 2010, *Brain, Body and Machine*, Springer Berlin Heidelberg, pp. 299-310. ISBN 978-3-642-16258-9

[7] Grand, C., Benamar, F., Plumet, F., and Bidaud, P., 2004, "Stability and traction optimization of a reconfigurable wheel-legged robot," The International Journal of Robotics Research, **23**(10-11), pp. 1041-1058. DOI: 10.1177/0278364904047616

[8] Adachi, H., and Koyachi, N., 2001, "Development of a leg-wheel hybrid mobile robot and its step-passing algorithm," *Intelligent Robots and Systems, 2001. Proceedings. 2001 IEEE/RSJ International Conference on*, IEEE, **2**, pp. 728-733. DOI: 10.1109/IROS.2001.976255

[9] Endo, G., and Hirose, S., 2012, "Study on roller-walker—improvement of locomotive efficiency of quadruped robots by passive wheels," Advanced Robotics, **26**(8-9), pp. 969-988. DOI: 10.1163/156855312X633066

[10] Thomson, T., Sharf, I., and Beckman, B., 2012, "Kinematic control and posture optimization of a redundantly actuated quadruped robot," *Robotics and Automation (ICRA), 2012 IEEE International Conference on*, IEEE, pp. 1895-1900. DOI: 10.1109/ICRA.2012.6224927

[11] Wilcox, B., H., "ATHLETE: A limbed vehicle for solar system exploration," 2012, *Aerospace Conference, 2012 IEEE*, IEEE, pp. 1-9. DOI: 10.1109/AERO.2012.6187269

[12] Tanaka, T., and Hirose, S., 2008, "Development of leg-wheel hybrid quadruped "AirHopper" design of powerful light-weight leg with wheel," *2008 IEEE/RSJ International Conference on Intelligent Robots and Systems*, IEEE, pp. 3890-3895. DOI: 10.1109/IROS.2008.4650880

[13] Huang, B., Wang, P., and Sun, L., 2006, "Behavior-based Control of a Hybrid Quadruped Robot," *2006 6th World Congress on Intelligent Control and Automation*, IEEE, **2**, pp. 8997-9001. DOI: 10.1109/WCICA.2006.1713740

[14] Luo, Y., Li, Q., and Liu, Z., 2014, "Design and optimization of wheel-legged robot: Rolling-Wolf," Chinese Journal of Mechanical Engineering, **27**(6), pp. 1133-1142. DOI: 10.3901/CJME.2014.0905.144

[15] Nakajima, S., 2011, "RT-Mover: a rough terrain mobile robot with a simple leg–wheel hybrid mechanism," The International Journal of Robotics Research, **30**(13), pp. 1609-1626. DOI: 10.1177/0278364911405697

[16] Yuan, J., and Hirose, S., 2004, "Research on leg-wheel hybrid stair-climbing robot, Zero Carrier," *Robotics and Biomimetics, 2004. ROBIO 2004. IEEE International Conference on*, IEEE, pp. 654-659. DOI: 10.1109/ROBIO.2004.1521858

[17] Szrek, J., Wójtowicz, P., 2010, "Idea of wheel-legged robot and its control system design," Bulletin of the Polish Academy of Sciences: Technical Sciences, **58**(1), pp. 43-50. DOI: 10.2478/v10175-010-0004-8

[18] Xu, K., and Ding, X., 2013, "Typical gait analysis of a six-legged robot in the context of metamorphic mechanism theory," Chinese Journal of Mechanical Engineering, **26**(4), pp. 771-783. DOI: 10.3901/CJME.2013.04.771

[19] Ding, X., Li, K., and Xu, K., 2012, "Dynamics and wheel's slip ratio of a wheel-legged robot in wheeled motion considering the change of height," Chinese Journal of Mechanical Engineering, **25**(5), pp. 1060-1067. DOI: 10.3901/CJME.2012.05.1060

[20] Guo, L., Chen, K., Zhao, D., Wu, D., Liu, Z., and Bing, Y., 2009, "Study on a wheel-legged hybrid mobile robot," Manufacturing Automation, **31**(10), pp. 1-6. (in Chinese)

[21] Lu, D., Dong, E., Liu, C., Xu, M., and Yang, J., 2016, "Generation and Analyses of the Reinforced Wave Gait for a Mammal-Like Quadruped Robot," Journal of Intelligent & Robotic Systems, **82**(1), pp. 51-68. DOI 10.1007/s10846-015-0265-4

[22] Zhang, L., Yang, Y., Gu, Y., Sun, X., Yao, X., and Shuai, L., 2016, "A New Compact Stair-Cleaning Robot," Journal of Mechanisms and Robotics, **8**(4), pp. 045001. DOI: 10.1115/1.4032700

[23] Lacagnina, M., Muscato, G., and Sinatra, R., 2003, "Kinematics, dynamics and control of a hybrid robot Wheeleg," Robotics and Autonomous Systems, **45**(3), pp. 161-180. DOI: 10.1016/j.robot.2003.09.006

[24] Ottaviano, and E., Rea, P., 2013, "Design and operation of a 2-DOF leg–wheel hybrid robot," Robotica, **31**(8), pp. 1319-1325. DOI: 10.1017/S0263574713000556

[25] Bruzzone, L., and Fanghella, P., 2016, "Functional Redesign of Mantis 2.0, a Hybrid Leg-Wheel Robot for Surveillance and Inspection," Journal of Intelligent & Robotic Systems, **81**(2), pp. 215-230. DOI: 10.1007/s10846-015-0240-0

[26] Boxerbaum, A., S., Klein, M., A., Bachmann, R., Quinn, R., D., Harkins, R., and Vaidyanathan, R., 2009, "Design of a semi-autonomous hybrid mobility surf-zone robot," *2009 IEEE/ASME International Conference on Advanced Intelligent Mechatronics*, IEEE, pp. 974-979. DOI: 10.1109/AIM.2009.5229713

[27] Hong, D., Jeans, J., B., and Ren, P., 2009, "Experimental verification of the walking and turning gaits for a two-actuated spoke wheel robot," *2009 IEEE/RSJ International Conference on Intelligent Robots and Systems*, IEEE, pp. 402-403. DOI: 10.1109/IROS.2009.5354275

[28] Herbert, S., D., Drenner, A., and Papanikolopoulos, N., 2008, "Loper: A quadruped-hybrid stair climbing robot," *Robotics and Automation, 2008. ICRA 2008. IEEE International Conference on*, IEEE, pp. 799-804. DOI: 10.1109/ROBOT.2008.4543303

[29] Eich, M., Grimminger, F., Bosse, S., Spenneberg, D., Kirchner, F., 2008, "Asguard: A Hybrid-Wheel Security and SAR-Robot Using Bio-Inspired Locomotion for Rough Terrain," *International Workshop on Robotics for Risky Interventions & Surveillance of Environment*, Benicàssim Spain.

[30] Kim, Y., S., Jung, G., P., Kim, H., Cho, K., J., and Chu, C., N., 2014, "Wheel Transformer: A Wheel-Leg Hybrid Robot with Passive Transformable Wheels," IEEE Transactions on Robotics, **30**(6), pp. 1487-1498. DOI: 10.1109/TRO.2014.2365651

[31] Chen, S., C., Huang, K., J., Chen, W., H., Shen, S., Y., Li, C., H., and Liu, P., C., 2014, "Quattroped: A Leg--Wheel Transformable Robot," IEEE/ASME Transactions on Mechatronics, **19**(2), pp. 730-742. DOI: 10.1109/TMECH.2013.2253615

[32] Chen, W., H., Lin, H., S., and Lin, P., C., 2014, "TurboQuad: A leg-wheel transformable robot using bio-inspired control," *2014 IEEE International Conference on Robotics and Automation (ICRA)*, IEEE, pp. 2090-2090. DOI: 10.1109/ICRA.2014.6907143

[33] Rohmer, E., Reina, G., Ishigami, G., Nagatani, K., and Yoshida, K., 2008, "Action planner of hybrid leg-wheel robots for lunar and planetary exploration," *2008 IEEE/RSJ International Conference on Intelligent Robots and Systems*, IEEE, pp. 3902-3907. DOI: 10.1109/IROS.2008.4651134

[34] Okada, T., Mahmoud, A., Botelho, W., T., and Shimizu, T., 2012, "Trajectory estimation of a skid-steering mobile robot propelled by independently driven wheels," Robotica, **30**(1), pp. 123-132. DOI: http://dx.doi.org/10.1017/S026357471100035X

[35] Tadakuma, K., Tadakuma, R., Maruyama, A., Rohmer, E., Nagatani, K., Yoshida, K., Ming, A., Shimojo, M., Higashimori, M., and Kaneko, M., 2010, "Mechanical design of the wheel-leg hybrid mobile robot to realize a large wheel diameter," *Intelligent Robots and Systems (IROS), 2010 IEEE/RSJ International Conference on*, IEEE, pp. 3358-3365. DOI: 10.1109/IROS.2010.5651912

[36] She, Y., Hurd, C., J., and Su, H., J., 2015, "A transformable wheel robot with a passive leg," *Intelligent Robots and Systems (IROS), 2015 IEEE/RSJ International Conference on*, IEEE, pp. 4165-4170. DOI: 10.1109/IROS.2015.7353966

[37] Bryson, J., T., Jin, X., and Agrawal, S., K., 2016, "Optimal design of cable-driven manipulators using particle swarm optimization," Journal of Mechanisms and Robotics, **8**(4), pp. 041003. DOI: 10.1115/1.4032103

[38] Spröwitz, A., T., Ajallooeian, M., Tuleu, A., and Ijspeert, A., J., 2014, "Kinematic primitives for walking and trotting gaits of a quadruped robot with compliant legs," Frontiers in computational neuroscience, **8**. DOI: 10.3389/fncom.2014.00027

[39] Tsusaka, Y., and Ota, Y., 2006, "Wire-driven bipedal robot," *2006 IEEE/RSJ International Conference on Intelligent Robots and Systems*, IEEE, pp. 3958-3963. DOI: 10.1109/IROS.2006.281831

[40] Zhong, Y., Li, Z., and Du, R., 2013, "The design and prototyping of a wire-driven robot fish with pectoral fins," *Robotics and Biomimetics (ROBIO), 2013 IEEE International Conference on*, IEEE, pp. 1918-1923. DOI: 10.1109/ROBIO.2013.6739749

[41] Zhang, K., Qiu, C., and Dai, J., S., 2016, "An Extensible Continuum Robot With Integrated Origami Parallel Modules," Journal of Mechanisms and Robotics, **8**(3): 031010. DOI: 10.1115/1.4031808

[42] Gravagne, I., A., Rahn, C., D., and Walker, I., D., 2003, "Large deflection dynamics and control for planar continuum robots," IEEE/ASME transactions on mechatronics, **8**(2), pp. 299-307. DOI: 10.1109/TMECH.2003.812829

[43] Webster, R., J., and Jones, B., A., 2010, "Design and kinematic modeling of constant curvature continuum robots: A review," The International Journal of Robotics Research, **29**(13), pp. 1661-1683. DOI: 10.1177/0278364910368147

[44] Burgner-Kahrs, J., Rucker, D., C., and Choset, H., 2015, "Continuum robots for medical applications: A survey," IEEE Transactions on Robotics, **31**(6), pp. 1261-1280. DOI: 10.1109/TRO.2015.2489500

[45] Kato, T., Okumura, I., Song, S., E., Golby, A., J., and Hata, N., 2015, "Tendon-Driven Continuum Robot for Endoscopic Surgery: Preclinical Development and Validation of a Tension Propagation Model," IEEE/ASME Transactions on Mechatronics, **20**(5), pp. 2252-2263. DOI: 10.1109/TMECH.2014.2372635

[46] Yang, Y., Chen, Y., Li, Y., and Chen, M., Z., 2016, "3D printing of variable stiffness hyper-redundant robotic arm," *2016 IEEE International Conference on Robotics and Automation (ICRA)*, IEEE, pp. 3871-3877. DOI: 10.1109/ICRA.2016.7487575

[47] Hyun, D., J., Seok, S., Lee, J., and Kim, S., 2014, "High speed trot-running: Implementation of a hierarchical controller using proprioceptive impedance control on the MIT Cheetah," The International Journal of Robotics Research, **33**(11), pp. 1417-1445. DOI: 10.1177/0278364914532150

[48] Weinmeister, K., Eckert, P., Witte, H., and Ijspeert, A., J., 2015, "Cheetah-cub-S: Steering of a quadruped robot using trunk motion," *2015 IEEE International Symposium on Safety, Security, and Rescue Robotics (SSRR)*, IEEE, pp. 1-6. DOI: 10.1109/SSRR.2015.7443021

[49] Khoramshahi, M., Sprowitz, A., Tuleu, A., Ahmadabadi, M., N., and Ijspeert, A., J., 2013, "Benefits of an active spine supported bounding locomotion with a small compliant quadruped robot," *Proceedings of 2013 IEEE International Conference on Robotics and Automation*, IEEE. DOI: 10.1109/ICRA.2013.6631041

[50] Eckert, P., Spröwitz, A., Witte, H., and Ijspeert, A., J., 2015, "Comparing the effect of different spine and leg designs for a small bounding quadruped robot," *2015 IEEE International Conference on Robotics and Automation (ICRA)*. IEEE, pp. 3128-3133. DOI: 10.1109/ICRA.2015.7139629

[51] Zhao, Q., Nakajima, K., Sumioka, H., Hauser, H., and Pfeifer, R., 2013, "Spine dynamics as a computational resource in spine-driven quadruped locomotion," *2013 IEEE/RSJ International Conference on Intelligent Robots and Systems*, IEEE, pp. 1445-1451. DOI: 10.1109/IROS.2013.6696539

[52] Zhang, X., L., Duan, G., H., Zheng, H., J., Zhao, L., Y., and Cheng, Z., F., 2003, "Bionic design of the quadrupedal robot and motion simulation," *Robotics, Intelligent Systems and Signal Processing, 2003. Proceedings. 2003 IEEE International Conference on*, IEEE, pp. 137-141. DOI: 10.1109/RISSP.2003.1285563

Journal of Mechanisms and Robotics. Received October 20, 2016;
Accepted manuscript posted June 9, 2017. doi:10.1115/1.4037018

Figure Captions List

Fig. 1 Prototype of *Transleg* in the (A) legged and (B) wheeled modes

Fig. 2 Schematic diagram of the leg-wheel mechanism in the (A) legged and (B) wheeled modes, and the numbers denote: ① body, ② hip joint, ③ actuator 1, ④ thigh, ⑤ rim, ⑥ spoke, ⑦ knee joint, ⑧ shank, ⑨ docking assembly, ⑩ thrust ball bearing, ⑪ torsion spring, ⑫ turnplate, ⑬ actuator 2, ⑭ wire, ⑮ hole, ⑯ rotary assembly, ⑰ foot, ⑱ bearing pedestal, ⑲ flange bearing, ⑳ dowel

Fig. 3 Schematic diagram of the spine mechanism, and the numbers denote: ① pitch actuator, ② front body, ③ pitch turnplate, ④ wire, ⑤ tail end, ⑥ spine joints, ⑦ yaw actuator, ⑧ rear body, ⑨ yaw turnplate, ⑩ head end, ⑪ vertebra, ⑫ silicon piece, ⑬ ball joints

Fig. 4 Geometries of leg-wheel mechanism for explaining (A) the relation between the rotation angle of turnplate and the angle of knee joint, (B) the angles of hip joint in anterior extreme position and posterior extreme position, and (C) the angle of knee joint in the wheeled mode

Fig. 5 Geometries of spine mechanism for explaining (1) the relation between the bending angle of *Transleg* in the yaw direction and the rotation angle of the yaw actuator, and (2) the relation between the bending angle of *Transleg* in the pitch direction and the rotation angle of the pitch actuator

Fig. 6 Control signals actuating *Transleg* to perform legged and wheeled

locomotion and switch between the two locomotion modes (FLH, FRH, HLH and HRH respectively denote hip joint of front-left, front-right, hind-left and hind-right leg-wheel; FLK, FRK, HLK and HRK respectively denote knee joint of front-left, front-right, hind-left and hind-right leg-wheel.)

Fig. 7 Snapshots of *Transleg* performing legged, wheeled and transformation motion in the simulation (the video can be found at VideoLink)

Fig. 8 Snapshots of *Transleg* performing legged, wheeled and transformation motion in the experiment (the video can be found at VideoLink)

Fig. 9 Relations between the bending angles of spine joints in yaw and pitch directions and the rotation angles of actuators, the increments and decrements of wire in the spine joints, and the length of wire let out by the yaw actuator and the pitch actuator (solid lines and dotted lines are respectively according to the left and right coordinates)

Fig. 10 Snapshots of *Transleg* performing spine motion (the video can be found at VideoLink)

Table Caption List

Journal of Mechanisms and Robotics. Received October 20, 2016;
Accepted manuscript posted June 9, 2017. doi:10.1115/1.4037018

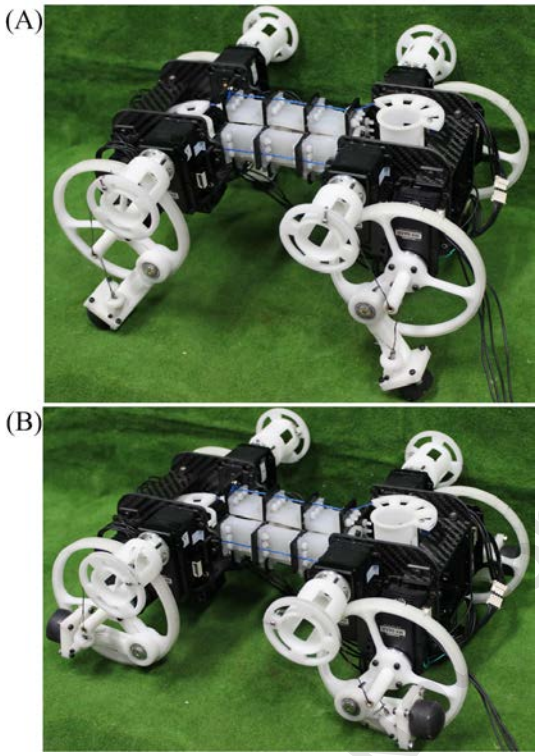

Fig. 1 Prototype of *Transleg* in the (A) legged and (B) wheeled modes

Journal of Mechanisms and Robotics. Received October 20, 2016;
Accepted manuscript posted June 9, 2017. doi:10.1115/1.4037018

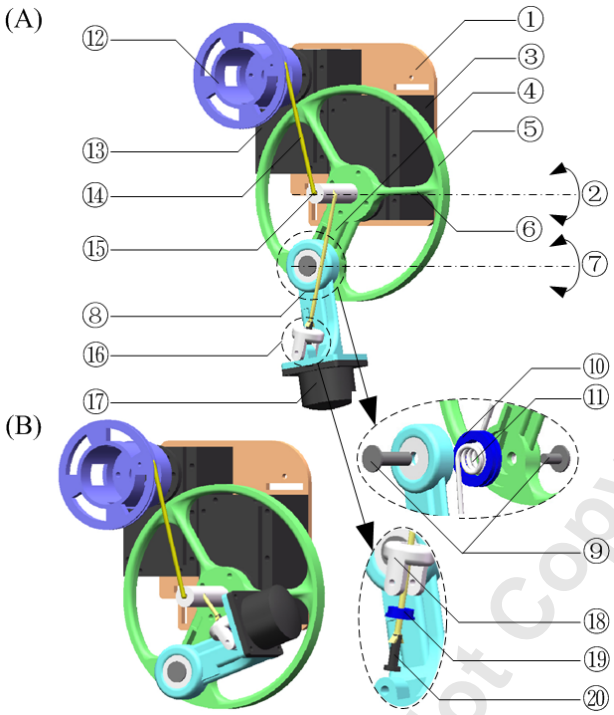

Fig. 2 Schematic diagram of the leg-wheel mechanism in the (A) legged and (B) wheeled modes. The numbers denote: ① body, ② hip joint, ③ actuator 1, ④ thigh, ⑤ rim, ⑥ spoke, ⑦ knee joint, ⑧ shank, ⑨ docking assembly, ⑩ thrust ball bearing, ⑪ torsion spring, ⑫ turnplate, ⑬ actuator 2, ⑭ wire, ⑮ hole, ⑯ rotary assembly, ⑰ foot, ⑱ bearing pedestal, ⑲ flange bearing, ⑳ dowel

Journal of Mechanisms and Robotics. Received October 20, 2016;
Accepted manuscript posted June 9, 2017. doi:10.1115/1.4037018

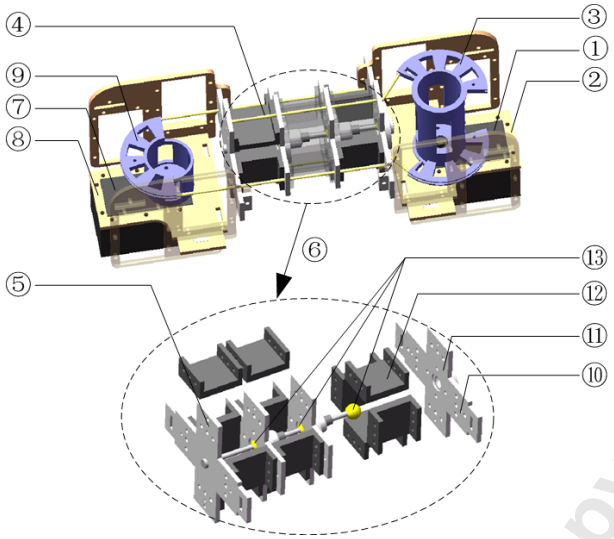

Fig. 3 Schematic diagram of the spine mechanism. The numbers denote: ① pitch actuator, ② front body, ③ pitch turnplate, ④ wire, ⑤ tail end, ⑥ spine joints, ⑦ yaw actuator, ⑧ rear body, ⑨ yaw turnplate, ⑩ head end, ⑪ vertebra, ⑫ silicon piece, ⑬ ball joints

Journal of Mechanisms and Robotics. Received October 20, 2016;
Accepted manuscript posted June 9, 2017. doi:10.1115/1.4037018

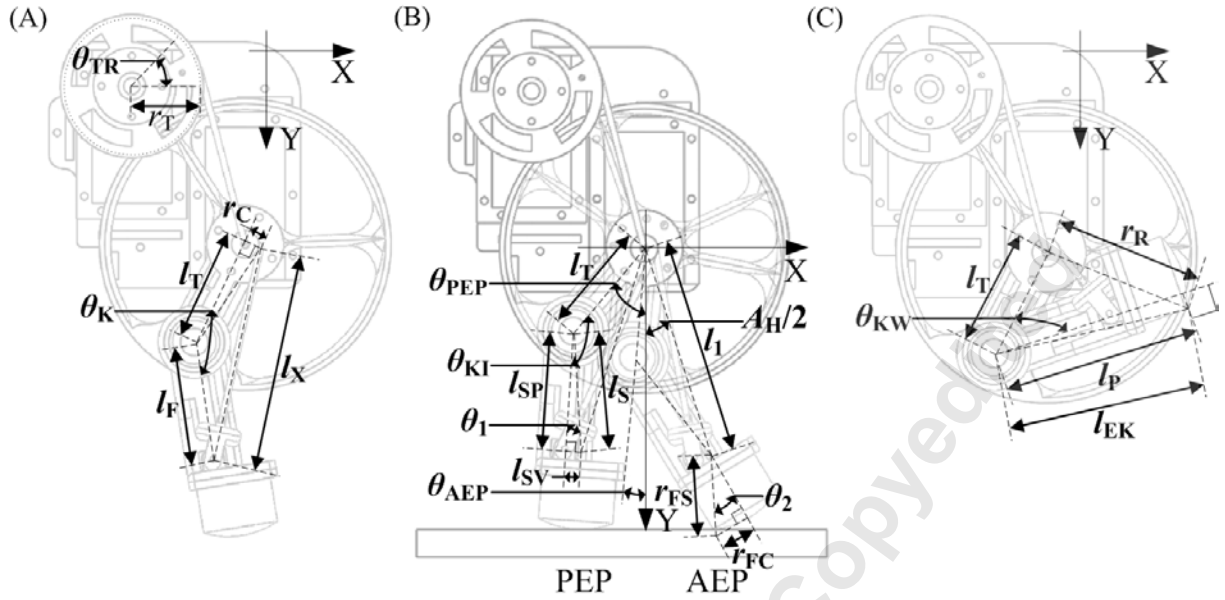

Fig. 4 Geometries of leg-wheel mechanism for explaining (A) the relation between the rotation angle of turnplate and the angle of knee joint, (B) the angles of hip joint in anterior extreme position and posterior extreme position, and (C) the angle of knee joint in the wheeled mode

Journal of Mechanisms and Robotics. Received October 20, 2016;
Accepted manuscript posted June 9, 2017. doi:10.1115/1.4037018

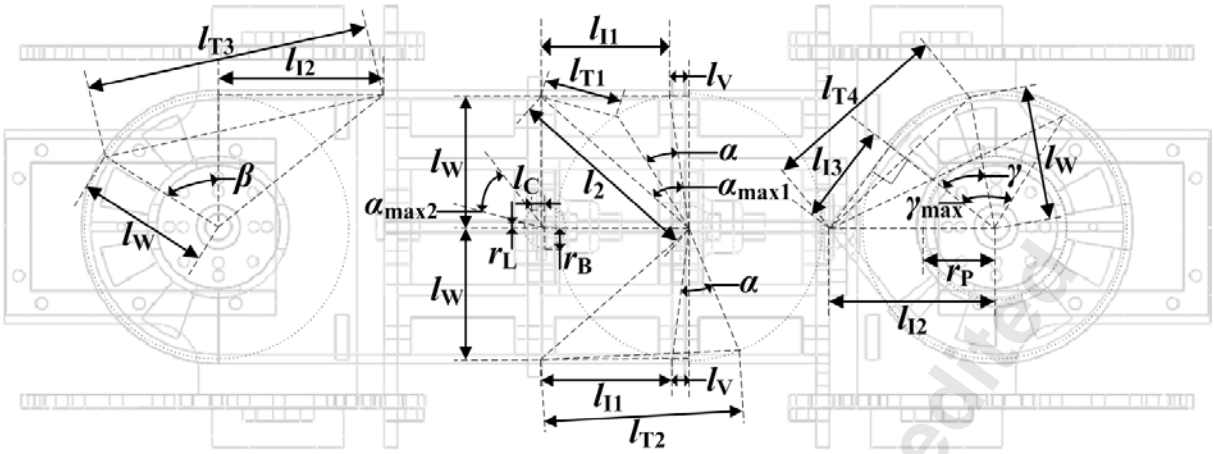

Fig. 5 Geometries of spine mechanism for explaining (1) the relation between the bending angle of *Transleg* in the yaw direction and the rotation angle of the yaw actuator, and (2) the relation between the bending angle of *Transleg* in the pitch direction and the rotation angle of the pitch actuator

Journal of Mechanisms and Robotics. Received October 20, 2016;
Accepted manuscript posted June 9, 2017. doi:10.1115/1.4037018

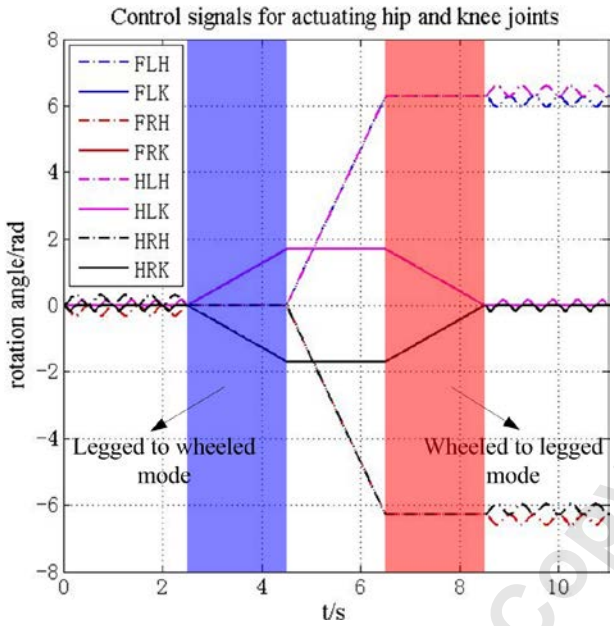

Fig. 6 Control signals actuating *Transleg* to perform legged and wheeled locomotion and switch between the two locomotion modes (FLH, FRH, HLH and HRH respectively denote hip joint of front-left, front-right, hind-left and hind-right leg-wheel; FLK, FRK, HLK and HRK respectively denote knee joint of front-left, front-right, hind-left and hind-right leg-wheel.)

Journal of Mechanisms and Robotics. Received October 20, 2016;
Accepted manuscript posted June 9, 2017. doi:10.1115/1.4037018

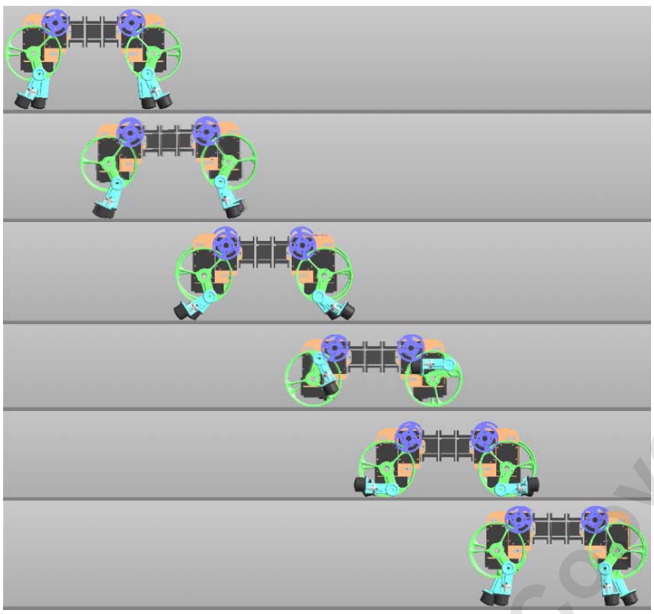

Fig. 7 Snapshots of *Transleg* performing legged, wheeled and transformation motion in the simulation (the video can be found at VideoLink)

Journal of Mechanisms and Robotics. Received October 20, 2016;
Accepted manuscript posted June 9, 2017. doi:10.1115/1.4037018

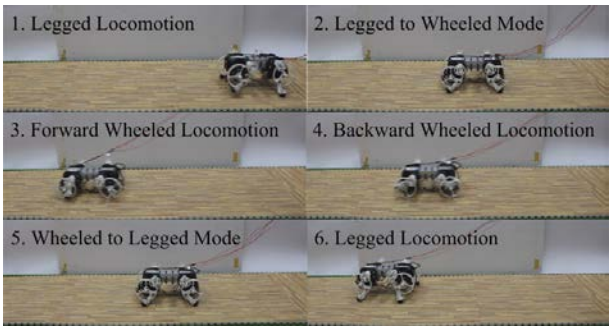

Fig. 8 Snapshots of *Transleg* performing legged, wheeled and transformation motion in the experiment (the video can be found at VideoLink)

Journal of Mechanisms and Robotics. Received October 20, 2016;
Accepted manuscript posted June 9, 2017. doi:10.1115/1.4037018

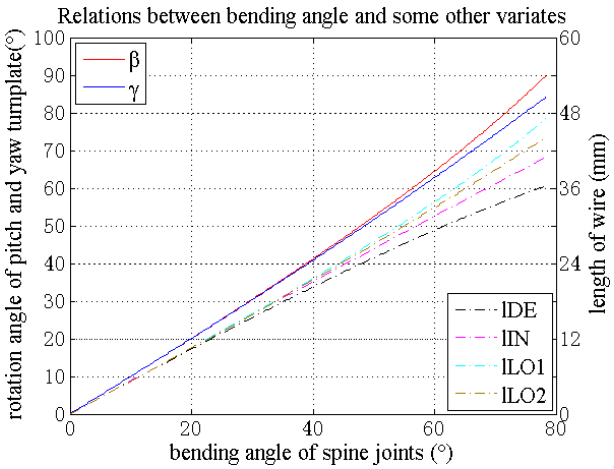

Fig. 9 Relations between the bending angles of spine joints in yaw and pitch directions and the rotation angles of actuators, the increments and decrements of wires in the spine joints, and the length of wire let out by the yaw actuator and the pitch actuator (solid lines and dotted lines are respectively according to the left and right coordinates)

Journal of Mechanisms and Robotics. Received October 20, 2016;
Accepted manuscript posted June 9, 2017. doi:10.1115/1.4037018

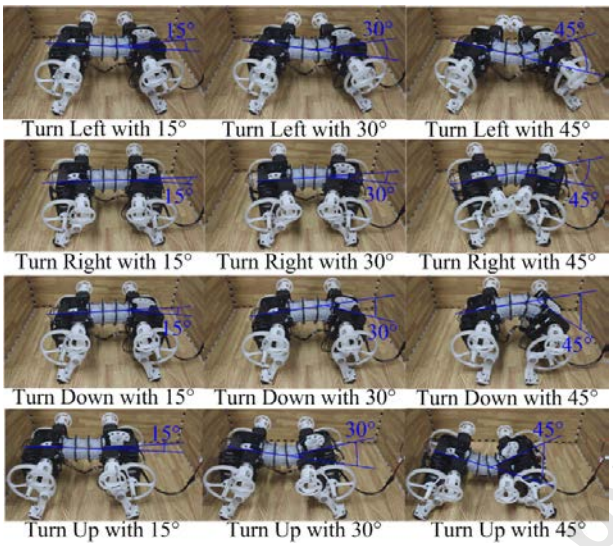

Fig. 10 Snapshots of *Transleg* performing spine motion (the video can be found at VideoLink)

Journal of Mechanisms and Robotics. Received October 20, 2016;
Accepted manuscript posted June 9, 2017. doi:10.1115/1.4037018

Table 1. Characteristics of some leg-wheel robots referenced in this paper and *Transleg*

Name	n_A	n_{LD}	n_{WD}
PAW [6]	2	1	1
Hylos [7]	4	2	2
Walk'n Roll [8]	2/3	1/3	0/1
Roller-Walker [9]	3	3	0
MHT [10]	3	2	1
Zero Carrier [16]	1/2	1	0/1
LegVan [17]	3/4	2	1/2
NOROS [18]	4	3	1
NOROS-Ⅱ [19]	3/4	3	0/1
IMPASS [27]	4	4	1
Loper [28]	1	1	1
Wheel Transformer [30]	1	1	1
Quattroped [31]	3	2	1
Turboquad [32]	2	2	1
LEON [33]	4	4	2
Transleg	**2**	**2**	**1**

Note: n_A denotes the number of actuators for each leg-wheel, n_{LD} denotes the number of active DOFs (degrees of freedom) for the leg, n_{WD} denotes the number of active DOFs for the wheel. "/" denotes "or", indicating the leg-wheels of the robot have different numbers of actuators or DOFs.

Table 2. Values of the geometries of *Transleg*

Name	r_C	l_T	l_F	r_T	l_S	l_{SP}	l_{SV}	r_{FC}	r_{FS}	l_{EK}
Value (mm)	5.00	40.00	43.00	24.20	40.58	40.13	6.00	13.50	31.87	69.41
Name	r_R	l_P	l_{I1}	l_V	l_W	l_C	r_B	r_L	l_{I2}	r_P
Value (mm)	53.00	69.00	29.56	4.00	30.00	3.00	4.80	1.50	37.66	16.00